Afyon Kocatepe Üniversitesi Fen ve Mühendislik Bilimleri Dergisi

Afyon Kocatepe University Journal of Science and Engineering

AKÜ FEMÜBİD **23** (2023) 041201 (874-882) AKU J. Sci. Eng. **23** (2023) 041201 (874-882)

DOI: 10.35414/ akufemubid.1256778

Araştırma Makalesi / Research Article

Improvement of Photocatalytic Degradation of Titanium Dioxide Nanomaterials by Non-metal Doping

Funda AK AZEM[1,2*], Isil BIRLIK[1,2], Ozgur Yasin KESKIN[1,3], Tulay KOC DELICE[3]

[1] Dokuz Eylul University, Department of Metallurgical and Materials Engineering, 35390, Buca, Izmir, Türkiye.

[2] Dokuz Eylul University, The Graduate School of Natural and Applied Sciences, Department of Nanoscience and Nanoengineering, 35390, Buca, Izmir, Türkiye.

[3] Dokuz Eylul University, The Graduate School of Natural and Applied Sciences, 35390, Buca, Izmir, Türkiye.

Corresponding author e-mail:funda.ak@deu.edu.tr ORCID ID: https://orcid.org/ 0000-0002-4446-1437*

e-mail: isil.kayatekin@deu.edu.tr ORCID ID: https://orcid.org/0000-0003-3098-2001

e-mail :ozgur.keskin@deu.edu.tr ORCID ID: https://orcid.org/0000-0003-4492-3360

e-mail: tulaykocdelice@gmail.com ORCID ID: https://orcid.org/0000-0003-3476-129X

Geliş Tarihi: 06.03.2023 Kabul Tarihi: 10.08.2023

Keywords

TiO_2; Sol-gel; Doping Non-metal; Photocatalytic activity

Abstract

Semiconductor photocatalysis is a process that benefits from sunlight to start chemical reactions. In order to take advantage photocatalytic properties of semiconductors and to achieve better performance structural adjustment is needed. In this study, varying amounts of nitrogen were used to modify TiO_2 nanostructures using the sol-gel method. The crystalline structure of the synthesized TiO_2 nanostructures was studied using the X-ray diffraction (XRD) technique. X-ray photoelectron spectroscopy (XPS) was conducted to analyse the elemental composition of nanomaterials. XPS analyze confirms that nitrogen is introduced into the lattice of TiO_2. The photocatalytic degradation of methylene blue (MB) under UV irradiation was employed to assess the photocatalytic performance of the samples. To evaluate degradation, the absorption of MB over time was measured using a UV-Vis spectrophotometer. As a result, the doping process has been found to improve the photocatalytic performance of TiO_2, and 0.2% N doped TiO_2 nanostructures demonstrated superior photocatalytic activity for photocatalytic degradation of MB.

Ametal Katkılama ile Titanyum Dioksit Nanomalzemelerin Fotokatalitik Bozunmasının İyileştirilmesi

Anahtar kelimeler

TiO_2; Sol-jel; Katkılama; Ametal; Fotokatalitik aktivite

Öz

Yarı iletken fotokataliz, kimyasal reaksiyonları başlatmak için güneş ışığından yararlanan bir süreçtir. Yarı iletkenlerin fotokatalitik özelliklerinden faydalanmak ve daha iyi performans elde etmek için yapısal düzenlemeye gereksinim duyulmaktadır. Bu çalışmada, sol-jel yöntemi kullanılarak TiO_2 nanoyapılarını değiştirmek için değişen miktarlarda nitrojen kullanılmıştır. Sentezlenen TiO_2 nanoyapıların kristal yapıları X-ışını kırınımı (XRD) yöntemiyle incelenmiştir. Nanomalzemelerin elemental bileşimini analiz etmek için X-ışını fotoelektron spektroskopisi (XPS) yapılmıştır. XPS analizi, nitrojenin TiO_2 kafesindeki varlığını doğrulamaktadır. Metilen mavisinin (MB) UV ışıması altında fotokatalitik bozunması, numunelerin fotokatalitik performansını değerlendirmek için kullanılmıştır. Bozulmayı değerlendirmek için, MB'nin 664 nm'de zaman içinde absorpsiyonu bir UV-Vis spektrofotometre kullanılarak ölçülmüştür. Sonuç olarak, katkılama işleminin TiO_2'nin fotokatalitik performansını iyileştirdiği ve %0,2 N katkılı TiO_2 nanoyapıların MB'nin fotokatalitik bozunmasında üstün fotokatalitik aktivite gösterdiği bulunmuştur.

1. Introduction

Recently, there has been great attention to developing photocatalysts, which are utilized in several applications and research fields, particularly in environmentally friendly and energy applications. Semiconductor photocatalyst benefits from sunlight for energy production and pollutant decomposition (Di Valentin *et al.* 2007, Suwannaruang *et al.* 2018). Semiconductor-based photocatalysts have been widely investigated due to their electronic arrangement to absorb exerted solar spectrum for photocatalytic reaction. Among semiconductors, titanium dioxide (TiO_2) has high photocatalytic activity and is commonly used because of its unique properties like chemical stability, inexpensiveness, oxidative power, and availability (Bashiri *et al.* 2017, Jaiswal *et al.* 2015). TiO_2 absorbs only UV light due to its broad band gap, which restricts its effectiveness in photocatalytic applications. Therefore, TiO_2 can utilize only 5% of the sunlight spectrum (Macwan *et al.* 2011, Cheng *et al.* 2012). Additionally, the recombination of photogenerated carriers is another reason that diminishes TiO_2's photocatalytic activity. Recently, studies in the literature have attempted to enhance TiO_2's photocatalytic activity by adjusting the band gap (Xu *et al.* 2019, Mironyuk *et al.* 2020, Al-Shehri *et al.* 2020). To improve the efficiency of TiO_2 under visible light, methods such as element doping, the development of semiconductor composite structures, and the introduction of template agents for the production or modification of TiO_2 structures could be employed. Among these approaches, doping TiO_2 by metal and non-metal ions promotes its photocatalytic performance (Lu *et al.* 2022). The addition of these metal and non-metal ions has an effect on the electronic structure of TiO_2 and broadens its absorbance capability to the visible light spectrum (Sanchez-Martinez *et al.* 2018, Marschall and Wang 2014, Xu *et al.* 2019). Many research and theoretical calculations indicate that non-metals such as carbon Irie *et al.* (2003), nitrogen Diwald *et al.* (2004), sulphur Ohno *et al.* (2004), boron Finazzi *et al.* (2008), and iodine Tojo *et al.* (2008) could be doped into TiO_2 to enhance its photocatalytic activity significantly (Asahi *et al.* 2001, Umebayashi *et al.* 2003). Nitrogen is the most effective and widely investigated element among non-metals because of its high electronegativity, high ionization energy, and similar radius to oxygen (Suwannaruang *et al.* 2018).

TiO_2 nanoparticles can be synthesized with various techniques like solvothermal method Yin *et al.* (2005), electrochemical method Lei *et al.* (2001), chemical vapour deposition Pradhan *et al.* (2003), hydrothermal method Andersson *et al.* (2002), microwave process Corradi *et al.* (2005), sonochemical method Yu *et al.* (2002), and sol-gel process Nithya *et al.* (2018). When compared to other methods, the sol-gel process is a well-established and widely used method for synthesizing nanoparticles. Sol-gel process contains hydrolysis and condensation process and the formation of gel which will form the crystalline structure of nanoparticles. Because sol-gel is a solution-based process, it has advantages with regard to homogeneity, suitability, flexibility, purity, and stoichiometry control (Keshmiri *et al.* 2004, Venkatachalam *et al.* 2007). According to the literature, many parameters such as analyte type, phase crystallinity, dopant content, and oxygen vacancies need to be considered in determining the best visible photocatalytic activity (Soares *et al.* 2011, OKata *et al.* 2005, Ihara *et al.* 2003). In this regard, studies on the amount of nitrogen doping are reviewed in the literature; however, a study on the photocatalytic impact of a wide range of N doping concentrations was not reported.

This study aims to use non-metal N doping to modify sol-gel derived TiO_2 and to investigate the influence of the doping process on photocatalytic performance. Structural assessment of prepared materials has been carried out by XRD, XPS and FTIR analysis. The degradation of Methylene Blue (MB) under visible light irradiation was done to determine the photocatalytic activity of the TiO_2 nanoparticles.

2. Materials and Methods

Undoped and N-doped TiO_2 nanoparticles were synthesized by using titanium (IV) isopropoxide (TTIP) (Aldrich, 97%) and urea (Sigma-Aldrich, ≥99.5%) as titanium and nitrogen sources,

respectively. Citric acid (Merck, ACS) has been used as a stabilizing agent. The sol-gel process was utilized to produce undoped and N-doped TiO_2 nanoparticles with variable nitrogen levels. TTIP was used to form a precursor solution, and different amounts of urea solutions were prepared in distilled water (H_2O:Ti molar ratio = 1: 0.18 %). Under stirring conditions, different amounts of urea solutions (N: Ti molar ratios of 0.1-1.6 %) were added to the precursor solution as a nitrogen source. Afterward, citric acid was added as a catalyst. The final solution was accomplished by mixing all the reactants for 2 hours (Heidolph MR Hei-Standard). Subsequently, nanoparticles were obtained by drying at 100°C followed by calcination at 550°C in air. Synthesized nanoparticles were named as TN0, TN1, TN2, TN3, TN4, and TN5, according to N to Ti molar percent ratio of 0, 0.1, 0.2, 0.4, 0.8, and 1.6, respectively. Investigation of crystal structures of undoped and doped TiO_2 nanoparticles was performed by using a Rigaku with Cu-K_α radiation in 2θ ranging from 3° to 90° with 4°/min scanning rate D/Max-2100/PC X-ray diffractometer. XPS (Thermo Scientific; Al-Kα 1350 eV) measurements were carried out to estimate the composition and chemical states of nanoparticles. XPS analysis of the samples was performed using an Al-Kα irradiation source with a beam size of 400 µm in diameter with a scanning number of 15. Particle size measurement of the nanostructures were conducted with Malvern Zeta Sizer Nano ZS90. The photocatalytic performance of the synthesized nanoparticles was studied via methylene blue degradation under UV light irradiation by UV lamp (UltraVitalux E27300 W, Osram). Produced samples were exposed to UV light for 1 hour at 15-minute intervals during the photocatalytic performance evaluation. After UV exposure with time intervals specified, absorption measurements were performed using a spectrophotometer (UV mini-1240, Shimadzu) at a wavelength of 664 nm.

3. Results and Discussion

Figure 1 depicts XRD patterns of TiO_2 nanoparticles with different amounts of nitrogen content. The diffraction peaks at 25.2°, 37.8°, 48.0°, 53.9°, 55.1°, 62.7°, 68.8°, 70.3°, 74.0°, and 76.1° correspond to anatase phase (JCPDS: 21-1273) planes (101), (004), (200), (105), (211), (204), (116), (220), (107), and (301), respectively (Sanchez-Martinez *et al.* 2018). According to the XRD patterns of synthesized nanoparticles, all of the samples show good crystallised structure related to the anatase phase. The diffraction at 2θ = 25.2° (101) is described as the characteristic peak of anatase crystal phase structure (Zhang *et al.* 2000). It is clear that incorporating nitrogen into the TiO_2 lattice inhibits crystalline growth in the calcination process, and this affects XRD peaks as a broadening at characteristic peak of anatase (101). It was determined that N doping had no detrimental impact on TiO_2 crystal phase structures.

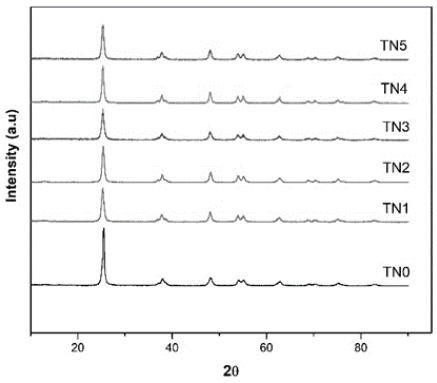

Figure 1. XRD patterns of TiO_2 specimens prepared with varying N-dopant contents

The average crystal size of the nanoparticles was estimated using the Full Width Half Maximum (FWHM) value at the peak (101) in the XRD patterns (Huang *et al.* 2006). Table 1 illustrates the crystalline size and particle sizes of nanoparticles. The crystalline size of undoped TiO_2 was 23.50 nm, whereas a significant reduction in crystalline size was observed with 0.4% nitrogen doping to TiO_2. Also, the broadening of peaks is in line with crystalline size reduction in N-doped TiO_2 nanoparticles.

Table 1. Crystalline size and particle size of TiO_2 nanoparticles

Sample Name	Crystalline size (nm)	Particle Size (nm)
TN0	23.50	68.70
TN1	13.95	90.7
TN2	15.75	52.67
TN3	14.93	37
TN4	18.5	65
TN5	16.3	64

A similar study conducted by Zhang and Liu (2008) shows that with increasing lanthanide content, average crystalline size decreased. This phenomenon is explained by the segregation of lanthanide ions in the grain boundary and restricting grain growth. Within this scope, it might be explained as a decrement in the crystalline size of TiO_2 connected to the nitrogen ions concentration in the grain boundary, which inhibit grain growth (Senthilnathan and Philip 2010). Figure 2 shows the average particle size distribution of doped TiO_2 nanoparticles. It is obviously seen that TN3 shows the lowest particle size with 37 nm and it is a threshold for particle size in terms of nitrogen content. According to the results, it was determined that all samples were successfully produced at the nanoscale and the particle sizes of the samples increased with increasing nitrogen content.

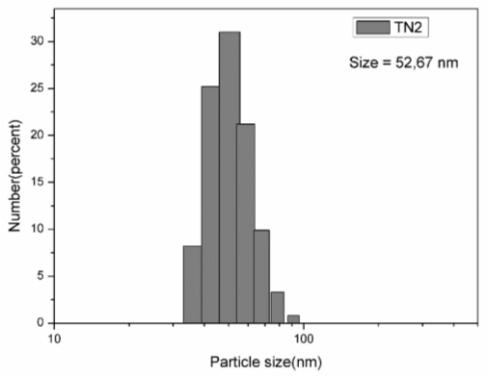

(a)

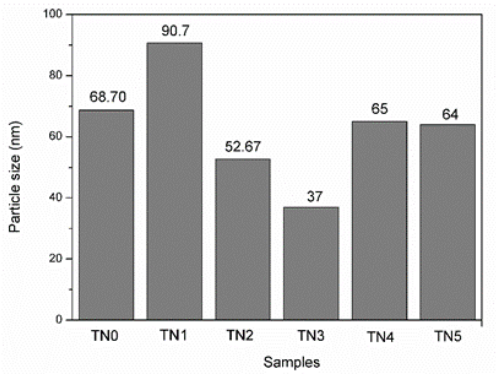

(b)

Figure 2. (a) Particle size distribution histogram of TN2, (b) measurements for undoped and doped TiO_2 nanoparticles.

XPS is a widespread method for assessing the elemental composition and electronic states of materials. To demonstrate N doping into the TiO_2 structure, XPS measurements of TN5 nanoparticles were conducted (Figure 3(a-e)). The survey spectrum obviously demonstrates Ti, O, N, and C peaks, as illustrated in Figure 3(a). The corresponding peaks associated with the Ti 2p O 1s and N 1s states revealed proof of the existence of Ti, O, and N elements, as shown in Figure 3(b-d). The peaks at 459.15 and 464.89 eV correlate to the binding energies of the Ti 2p3/2 and Ti 2p1/2 for the doped nanoparticles, respectively. This indicates the presence of titanium in the form of Ti4+ in the structure (Figure 3(c)). It is possible to deduce that using carbon bands during XPS analysis prompted the C1s peak at 284.6 eV to appear in the spectra (Jaiswal *et al.* 2012, Zhao 2008). Figures 3(c) and 3(d) display the XPS spectra of N 1s and O 1s for the doped TiO_2 samples, respectively. The location of the major peak at 531.5, which relates to the surface -OH bonds, is assigned to the O 1s core level (Figure 3(d)). N 1s peak at approximately 400 eV with low binding energy indicates that N successfully introduced into titanium dioxide. These findings are in agreement with previously reported studies using nitrogen as a dopant (Chen and Burda 2004, Li *et al.* 2015). Senthilnathan and Philip (2010) have reported that with nitrogen doping binding energy of Ti 2p states decreased. Different electrical interactions between Ti and N ions account for this decrease. These interactions result in an electron transition from N to Ti, resulting in an increase in electron density on Ti. The mechanism for the increase in electron density can be linked to nitrogen's weaker electronegativity compared to oxygen (Cong *et al.* 2007, Senthilnathan and Philip 2010). Figure 3(e) shows Ti 2p states of undoped (465 and 459.37 eV) and N-doped TiO_2 (464.88 and 459.18 eV) nanoparticles. Within reported studies, when comparing undoped and N-doped TiO_2 nanoparticles a decrease in the binding energy of doped TiO_2 nanostructure was observed. This change toward lower binding energy can be explained by nitrogen successfully incorporated into the TiO_2 lattice (Chen and Burda 2004, Jaiswal *et al.* 2012).

The photocatalytic degradation of samples has been determined by measuring the photodegradation of methylene blue under UV light irradiation for up to 60 min at 15-min intervals.

Degradation rate was determined using the formula (Equation 1),

$$\left(\frac{C_0 - C}{C_0}\right) x\ 100 \qquad (1)$$

where C_0 and C are the initial concentration of MB and the concentration after irradiation, respectively. The result was used to estimate the percentage of residual MB in the solution (Dariani *et al.* 2016). Figure 4 shows absorbance values the synhesized TiO_2 nanoparticles under methylene blue degradation with irradiation time. The photocatalytic efficiency of undoped and doped TiO_2 nanoparticles as a function of MB degradation is given in Figure 5.

According to these results, it is obvious that nitrogen doping has increased the photocatalytic activity of TiO_2 nanoparticles significantly. Substitutional N is widely referred to as responsible for band gap narrowing and enhancing visible photoactivity (Dawson *et al.* 2014). The findings showed that the absorbance peak of the 0.2% N-doped TiO_2 (TN2) demonstrated the fastest decrease within 60 min under UV light illuminations as seen in Figure 6.

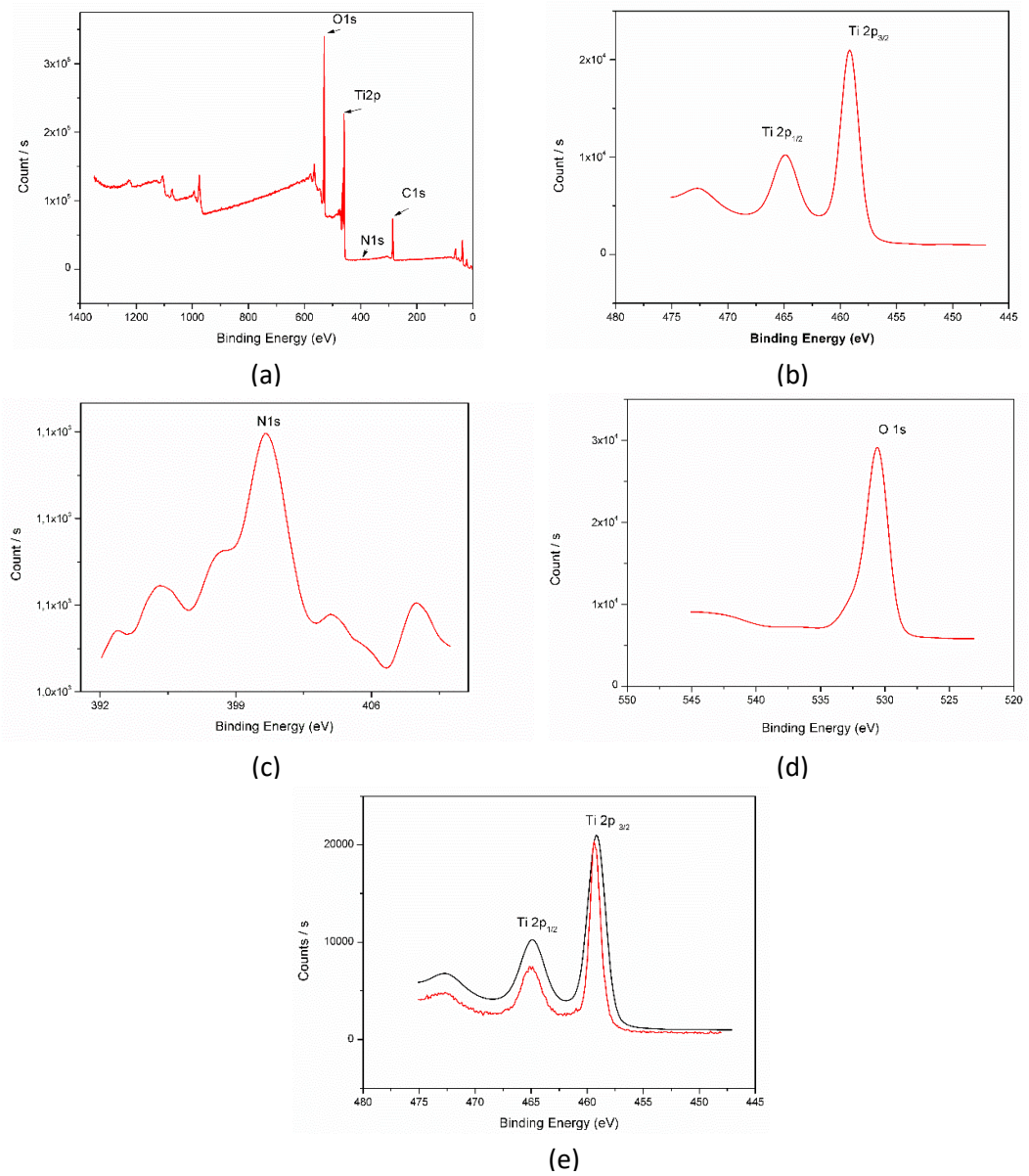

Figure 3. (a) Global XPS spectra of TN5,(b) Ti 2p spectra of TN5, (c) N 1s intensity peak of TN5, (d) O 1s spectra of TN5, and (e) Ti $2p_{3/2}$ and Ti $2p_{½}$ spectra of TN0 and TN5.

This result demonstrates that the nonmetal addition is the optimum doping solution in terms of photocatalytic performance. The rate of MB photodegradation increased as the amount of doping nitrogen increased, and the rate of degradation maximized at 0.2%. However, as the amount of dopants was increased further, the photodegradation rate was reduced. As stated in the literature, the recombination center of photogenerated carriers in TiO_2 will rise with excessive N doping, which is detrimental to the separation of photogenerated charge and diminishes the catalyst's photocatalytic activity. (Huang *et al.* 2021, Pawar *et al.* 2020).

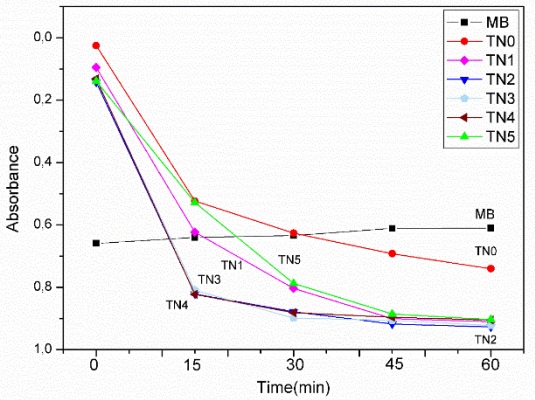

Figure 4. MB degradation with an irradiation time of synthesized undoped and doped TiO_2

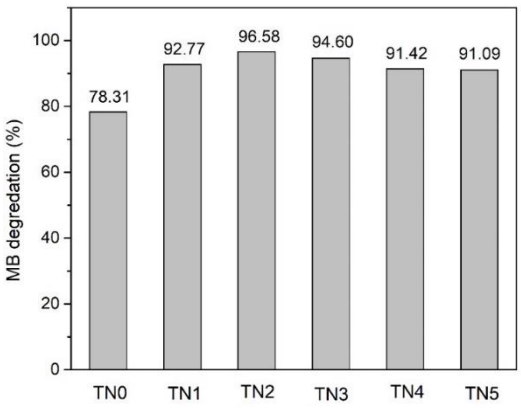

Figure 5. The photocatalytic efficiency of undoped and doped TiO_2 nanostructures as function MB degradation.

4. Conclusions

Nitrogen-doped TiO_2 nanoparticles were successfully synthesized with different nitrogen content by using the sol-gel route. The XRD pattern of all produced materials shows a pure anatase phase and the anatase (101) diffraction peak has been widened for nitrogen-doped nanoparticles.

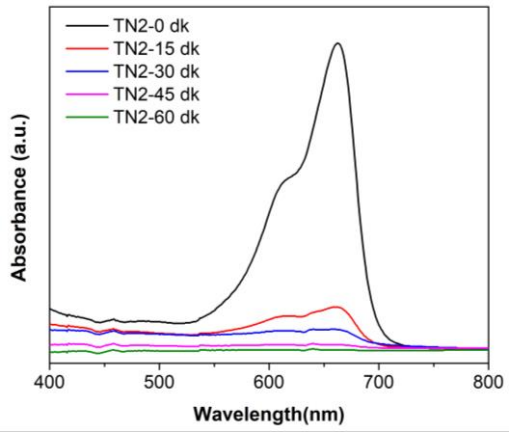

Figure 6. Absorbance spectrum of TN2 sample

This indicates that nitrogen was introduced into the TiO_2 lattice successfully. By comparing the crystal sizes of the samples, it was concluded that the crystal size of the samples decreased with the N doping process. The XPS examination of the nitrogen-incorporated nanoparticles provides a line at around to 400 eV, implying that N is displaced by O in the crystal structure as Ti-O-N. The photocatalytic efficiency of samples was evaluated with methylene blue degradation and with increasing nitrogen content. The TN2 sample with a molar ratio of 0.2% nitrogen displayed the greatest efficiency in terms of photocatalytic performance, and after this threshold value, the photocatalytic efficiency tended to decline in samples with increasing N content. It is possible to commercialize N-doped TiO_2 products for solving environmental problems such as candidate material for wastewater treatment applications and environment problems with improved photocatalytic properties

Acknowledgement

The financial support for this research was provided through Project No: 2020.KB.FEN.026 financed by Dokuz Eylul University Department of Scientific Research Projects. Additionally, the authors would like to thank Dogacan Dagdelen for his support.

5. References

Al-Shehri, B., Altass, H. M., Ashour, S. S., Shkir, M., Abd El Rahman, S. K. and Hamdy, M. S, 2020. Enhancement the photocatalytic performance of semiconductors

through composite formation with Eu-TUD-1. *Optik*, **202**, 163522.

Andersson, M., Österlund, L., Ljungström, S. and Palmqvist, A., 2002. Preparation of nanosize anatase and rutile TiO_2 by hydrothermal treatment of microemulsions and their activity for photocatalytic wet oxidation of phenol. *The Journal of Physical Chemistry B*, **106(41)**, 10674-10679.

Asahi, R., Morikawa, T. Ohwaki, T., Aoki, K. and Taga, Y., 2001. Visible-light photocatalysis in nitrogen-doped titanium oxides. *Science*, **293(5528)**, 269-271.

Bashiri, R., Mohamed, N. M. and Kait, C. F., 2017. Advancement of sol-gel-prepared TiO_2 photocatalyst. Recent Applications in Sol-Gel Synthesis, Usha Chandra, *Rijeka: InTech,* 151-167.

Chen, X. and Burda, C., 2004. Photoelectron spectroscopic investigation of nitrogen-doped titania nanoparticles. *The Journal of Physical Chemistry B*, **108(40)**, 15446-15449.

Cheng, X., Yu, X., Xing, Z. and Wan, J., 2012. Enhanced photocatalytic activity of nitrogen doped TiO_2 anatase nano-particle under simulated sunlight irradiation. *Energy Procedia*, **16**, 598-605.

Cong, Y., Zhang, J., Chen, F. and Anpo, M., 2007. Synthesis and characterization of nitrogen-doped TiO_2 nanophotocatalyst with high visible light activity. *The Journal of Physical Chemistry C*, **111(19)**, 6976-6982.

Corradi, A.B, Bondioli, F., Focher, B., Ferrari, A.M, Grippo, C., Mariani, E. and Villa, C., 2005. Conventional and Microwave-Hydrothermal Synthesis of TiO_2 Nanopowders. *Journal of the American Ceramic Society,* **88**, 2639-2641.

Dariani, R. S., Esmaeili, A., Mortezaali, A. and Dehghanpour, S., 2016. Photocatalytic reaction and degradation of methylene blue on TiO_2 nano-sized particles. *Optik*, **127(18)**, 7143-7154.

Dawson, M., Soares, G. B. and Ribeiro, C., 2014. Influence of calcination parameters on the synthesis of N-doped TiO_2 by the polymeric precursors method. *Journal of Solid State Chemistry*, **215**, 211-218.

Di Valentin, C., Finazzi, E., Pacchioni, G., Selloni, A., Livraghi, S., Paganini, M.C., Giamello, E., 2007. N-doped TiO_2: theory and experiment. *Chemical Physics,* **339**, 44-56.

Finazzi, E., Di Valentin, C. and Pacchioni, G., 2008. Boron-doped anatase TiO_2: pure and hybrid DFT calculations. *The Journal of Physical Chemistry C,* **113**, 220-228.

Irie, H., Watanabe, Y. and Hashimoto, K.,2003. Carbon-doped anatase TiO_2 powders as a visible-light sensitive photocatalyst. *Chemistry Letters*, **32(8)**, 772-773.

Huang, D. G., Liao, S. J., Liu, J. M., Dang, Z. and Petrik, L., 2006. Preparation of visible-light responsive N–F-codoped TiO_2 photocatalyst by a sol–gel-solvothermal method. *Journal of Photochemistry and Photobiology A*: Chemistry, **184(3)**, 282-288.

Huang, J., Dou, L., Li, J., Zhong, J., Li, M. and Wang, T., 2021. Excellent visible light responsive photocatalytic behavior of N-doped TiO_2 toward decontamination of organic pollutants. *Journal of Hazardous Materials*, **403**, 123857.

Ihara, T., Miyoshi, M., Iriyama, Y., Matsumoto, O. and Sugihara, S., 2003. Visible-light-active titanium oxide photocatalyst realized by an oxygen-deficient structure and by nitrogen doping. *Applied Catalysis B: Environmental*, **42(4)**, 403-409.

Jaiswal, R., Bharambe, J., Patel, N., Dashora, A., Kothari, D. C. and Miotello, A.,2015. Copper and Nitrogen co-doped TiO_2 photocatalyst with enhanced optical absorption and catalytic activity. *Applied Catalysis B: Environmental*, **168**, 333-341.

Jaiswal, R., Patel, N., Kothari, D. C. and Miotello, A., 2012. Improved visible light photocatalytic activity of TiO2 co-doped with Vanadium and Nitrogen. *Applied Catalysis B: Environmental*, **126**, 47-54.

Keshmiri, M., Mohseni, M. and Troczynski, T., 2004. Development of novel TiO_2 sol–gel-derived composite and its photocatalytic activities for trichloroethylene oxidation. *Applied Catalysis B: Environmental*, **53(4),** 209-219.

Lei, Y., Zhang, L. D. and Fan, J. C., 2001. Fabrication, characterization and Raman study of TiO2 nanowire arrays prepared by anodic oxidative hydrolysis of TiCl3. *Chemical Physics Letters*, **338(4-6),** 231-236.

Li, H., Hao, Y., Lu, H., Liang, L., Wang, Y., Qiu, J., ... and Yao, J., 2015. A systematic study on visible-light N-doped TiO_2 photocatalyst obtained from ethylenediamine by sol-gel method. *Applied Surface Science*, **344**, 112-118.

Lu, C. M., Sharma, R. K., Lin, P. Y., Huang, Y. H., Chen, J. S., Lee, W. C. and Chen, C. Y., 2022. Characteristics of Doped TiO2 Nanoparticle Photocatalysts Prepared by the Rotten Egg White. *Materials*, **15(12)**, 4231.

Macwan, D. P., Dave, P. N. and Chaturvedi, S., 2011. A review on nano-TiO_2 sol-gel type syntheses and its applications. *Journal of Materials Science*, **46**, 3669-3686.

Marschall, R. and Wang, L., 2014. Non-metal doping of transition metal oxides for visible-light photocatalysis. *Catalysis Today*, **225**, 111-135.

Mironyuk, I. F., Soltys, L. M., Tatarchuk, T. R. and Tsinurchyn, V. I., 2020. Ways to improve the efficiency of TiO_2-based photocatalysts. *Physics and Chemistry of Solid State*, **21(2)**, 300-311.

Nithya, N., Bhoopathi, G., Magesh, G. and Kumar, C. D. N., 2018. Neodymium doped TiO_2 nanoparticles by sol-gel method for antibacterial and photocatalytic activity. *Materials Science in Semiconductor Processing*, **83**, 70-82.

Diwald, O., Thompson, T. L., Goralski, E. G., Walck, S. D. and Yates, J. T., 2004. The effect of nitrogen ion implantation on the photoactivity of TiO_2 rutile single crystals. *The Journal of Physical Chemistry B*, **108(1)**, 52-57.

Okato, T., Sakano, T. and Obara, M., 2005. Suppression of photocatalytic efficiency in highly N-doped anatase films. *Physical Review B*, **72(11)**, 115124.

Pawar, M. J., Nimbalkar, V. B., Gaonar, M. D., Khajone, A. D. and Taywade, R. K., 2020. Effect of Nitrogen Doping on Photocatalytic Activity of TiO_2. *Journal of Nanoscience and Technology*, **6(4)**, 918-923.

Pradhan, S. K., Reucroft, P. J., Yang, F. and Dozier, A., 2003. Growth of TiO_2 nanorods by metalorganic chemical vapor deposition. *Journal of Crystal Growth*, **256(1-2)**, 83-88.

Tojo, S., Tachikawa, T., Fujitsuka, M. and Majima, T., 2008. Iodine-doped TiO_2 photocatalysts: correlation between band structure and mechanism. *The Journal of Physical Chemistry C*, **112(38)**, 14948-14954.

Sanchez-Martinez, A., Ceballos-Sanchez, O., Koop-Santa, C., López-Mena, E. R., Orozco-Guareño, E. and García-Guaderrama, M., 2018. N-doped TiO_2 nanoparticles obtained by a facile coprecipitation method at low temperature. *Ceramics International*, **44(5)**, 5273-5283.

Senthilnathan, J. and Philip, L., 2010. Photocatalytic degradation of lindane under UV and visible light using N-doped TiO_2. *Chemical Engineering Journal*, **161(1-2)**, 83-92.

Soares, G. B., Bravin, B., Vaz, C. M. and Ribeiro, C., 2011. Facile synthesis of N-doped TiO_2 nanoparticles by a modified polymeric precursor method and its photocatalytic properties. *Applied Catalysis B: Environmental*, **106(3-4)**, 287-294.

Suwannaruang, T., Kamonsuangkasem, K., Kidkhunthod, P., Chirawatkul, P., Saiyasombat, C., Chanlek, N. and Wantala, K., 2018. Influence of nitrogen content levels on structural properties and photocatalytic activities of nanorice-like N-doped TiO_2 with various calcination temperatures. *Materials Research Bulletin*, **105**, 265-276.

Ohno, T., Akiyoshi, M., Umebayashi, T., Asai, K., Mitsui, T. and Matsumura, M., 2004. Preparation of S-doped TiO_2 photocatalysts and their photocatalytic activities under visible light. *Applied Catalysis A: General*, **265(1)**, 115-121.

Umebayashi, T., Yamaki, T., Tanaka, S. and Asai, K., 2003. Visible light-induced degradation of methylene blue on S-doped TiO_2. *Chemistry Letters*, **32(4)**, 330-331.

Venkatachalam, N., Palanichamy, M. and Murugesan, V., 2007. Sol-gel preparation and characterization of nanosize TiO_2: Its photocatalytic performance. *Materials Chemistry and Physics*, **104(2-3)**, 454-459.

Xu, T., Wang, M. and Wang, T., 2019. Effects of N doping on the microstructures and optical properties of TiO_2. *Journal of Wuhan University of Technology-Mater. Sci. Ed.*, **34(1)**, 55-63.

Yin, S., Aita, Y., Komatsu, M., Wang, J., Tang, Q. and Sato, T., 2005. Synthesis of excellent visible-light responsive $TiO_{2-x}N_y$ photocatalyst by a homogeneous

precipitation-solvothermal process. *Journal of Materials Chemistry*, **15(6)**, 674-682.

Yu, J. C., Yu, J., Ho, W., Jiang, Z. and Zhang, L., 2002. Effects of F-doping on the photocatalytic activity and microstructures of nanocrystalline TiO_2 powders. *Chemistry of Materials*, **14(9)**, 3808-3816.

Zhang, Q., Gao, L. and Guo, J., (2000. Effects of calcination on the photocatalytic properties of nanosized TiO_2 powders prepared by $TiCl_4$ hydrolysis. *Applied Catalysis B: Environmental*, **26(3)**, 207-215.

Zhao, Y., Qiu, X. and Burda, C., 2008. The effects of sintering on the photocatalytic activity of N-doped TiO_2 nanoparticles. *Chemistry of Materials*, **20(8)**, 2629-2636.

Zhao, Z. and Liu, Q., 2008. Effects of lanthanide doping on electronic structures and optical properties of anatase TiO_2 from density functional theory calculations. *Journal of Physics D: Applied Physics*, **41**, 085417.